# Cubic Symmetry Effects in Solid $He^3$†*

DAVID ROSENWALD‡
*Department of Physics, University of California, San Diego, La Jolla, California*
(Received 12 May 1966; revised manuscript received 14 September 1966)

A detailed analysis is made of the single-particle model for solid $He^3$ at 0°K under an external pressure of 30 atm. The correct Hamiltonian being assumed, it is shown at the outset that the calculation gives a rigorous upper bound for the ground-state enthalpy of the system. The many-body wavefunction is taken to be a product of single-particle wave functions which are cubically symmetric about their respective lattice sites. In order to obtain the best product wave function of this type, the usual minimization principles are applied, and a set of self-consistent equations are obtained which differ as expected from the spherically symmetric Hartree equations. These cubically symmetric equations are then solved numerically, and the ground-state energy obtained is 10% lower than that obtained in the spherically symmetric approximation. This result is still significantly higher than the probable experimental value.

## I. INTRODUCTION

In the past several years there has been considerable theoretical interest in the properties of solid $He^3$ at 0°K. Most prominent have been those calculations in which the many-body wave function is ultimately taken to be a product of single-particle wave functions (single-particle model),[1–5] and it is with a calculation of this type that we will be concerned in this work.

Unlike most solids which may be treated classically, with the application of quantum mechanics to explain the small deviations from classical theory, solid $He^3$ is a manifestly "quantum solid." Because of the small $He^3$ atomic mass and the relatively weak interaction between the $He^3$ atoms, the zero-point kinetic energy of solid $He^3$ is of the same order of magnitude as the potential energy and hence may not be treated as a perturbation on the classical potential energy. (In addition to requiring the use of quantum mechanics, this large zero-point energy results in an expansion of the system with the result that over 30 atm of pressure are required to solidify $He^3$ at absolute zero.) Moreover, because of marked anharmonicity, it is difficult to deal with the potential energy by the usual quantum-mechanical perturbation techniques. Hence, since neither the potential nor the kinetic energy may be easily treated by perturbation methods, the quantum solid $He^3$ presents us with an interesting theoretical problem.

In this work we give a detailed exposition of the single-particle model for this problem, emphasizing explicitly the effects of cubic symmetry but neglecting correlation effects although these are clearly important in the case of solid $He^3$. Our purpose is to present certain features of the theory in some detail and especially to show the effects of the "symmetry of the lattice." In Sec. II we review basic principles and assumptions, and in Sec. III we show how to obtain the best variational results using a many-body wave function which is a product of single-particle wave functions each of which is cubically symmetric about its own lattice site. This method allows us to obtain a rigorous upper bound for the true enthalpy of the system. In Sec. IV we give the results of our calculations and review the known experimental data. The computational methods used are given in Appendix B.

## II. BASIC PRINCIPLES AND ASSUMPTIONS

In general, to obtain the energy of a given system for temperature $T>0$, one must calculate several eigenstates, determine the probability of the system being in each state, and then use statistical averaging to determine the energy. At absolute zero, however, Planck's statement of the Nernst postulate[6] implies that there is one particular state of lower energy than any other, and it is this state alone which is occupied by the system at all times, i.e., at absolute zero the energy is simply

$$U(S=0, V)=U_0(V), \tag{2.1}$$

where $U_0(V)$ is the lowest energy state of the system of volume $V$. Let $\Phi(V)$ be the true wave function for this state, and let $\Psi(V)$ be any typical wave function which is used in calculation. Then it is well known that

$$U_0(V)\leq\tilde{U}_0(V), \tag{2.2}$$

where the quantity with the tilde refers to the energy calculated using the variational wave function $\Psi(V)$, and the quantity on the left refers to the true lowest energy which is obtained by using the true wavefunction $\Phi(V)$.

* Supported in part by contract with U. S. Atomic Energy Commission.
† Based on part of a thesis submitted by the author to the Department of Physics, University of California, San Diego, in partial satisfaction of requirements for the degree Doctor of Philosophy.
‡ Present address: Bell Telephone Laboratories, Incorporated, Whippany, New Jersey 07981.
[1] *Helium Three*, edited by J. G. Daunt (Ohio State University Press, Columbus, Ohio, 1960).
[2] N. Bernardes and D. F. Brewer, Rev. Mod. Phys. **34**, 190 (1962).
[3] N. Bernardes and H. Primakoff, Phys. Rev. **119**, 968 (1960).
[4] L. H. Nosanow and G. L. Shaw, Phys. Rev. **128**, 546 (1962).
[5] L. H. Nosanow, Phys. Rev. Letters **13**, 270 (1964).
[6] H. B. Callen, *Thermodynamics* (John Wiley & Sons, Inc., New York, 1960).

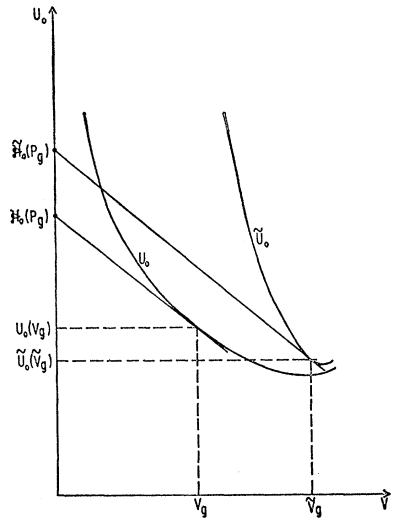


FIG. 1. Example of a possible case in which $\tilde{U}_0(\tilde{V}_g)<U_0(V_g)$ but $\tilde{\mathcal{H}}_0(P_g)>\mathcal{H}_0(P_g)$. See Sec. II for discussion.

Using Eq. (2.2) it is straightforward to show that the proper variational theorem to be used for systems under pressure $P$ at $T=0°K$ is

$$\mathcal{H}_0(P)\leq\tilde{\mathcal{H}}_0(P), \tag{2.3}$$

where $\mathcal{H}_0$ is the thermodynamic enthalpy at $T=0$, and $(-P)$ is defined as the volume derivative of the true and calculated energies, respectively.

The significance of Eq. (2.3) is described graphically in Fig. 1. It should be noted that for $P>0$ it is imperative to keep the pressure term in Eq. (2.3), for we can, in fact, have the situation shown in the figure where $\tilde{U}_0(\tilde{V}_g)<U_0(V_g)$, yet we still have $\tilde{\mathcal{H}}_0(P_g)>\mathcal{H}_0(P_g)$ which is consistent with Eq. (2.3). In the above, $V_g$ is the volume of the system under a given pressure $P_g$ and $T=0$, i.e.,

$$(-P_g)=\left.\frac{dU_0(V)}{dV}\right|_{V=V_g}=\left.\frac{d\tilde{U}_0(V)}{dV}\right|_{V=\tilde{V}_g}. \tag{2.4}$$

In addition to other assumptions which will be introduced as required, we use the following throughout this work:

(a) In accordance with experimental observation,[2] solid $He^3$ exists in bcc lattice form for pressures from 30–40 to 100–150 atm at $T=0°K$. (b) At $T=0°K$, the $He^3$ atom remains intact as a fermion with two paired electrons. (c) The Hamiltonian for the system is

$$H=\left(\frac{-\hbar^2}{2m}\right)\sum_{i=1}^{N}\nabla_i^2+\tfrac{1}{2}\sum_{ij}{}'v_{LJ}(r_{ij}), \tag{2.5}$$

where $N$ is the total number of atoms in the system,

$$\sum_{ij}{}'$$

has the usual significance that $i, j$ go from 1 to $N$ with the case $i=j$ excluded, and $v_{LJ}(r)$ is the Lennard-Jones potential

$$v_{LJ}(r)=4\epsilon[(\sigma/r)^{12}-(\sigma/r)^6], \tag{2.6}$$

where, for $He^3$, $\epsilon=10.22°K$ and $\sigma=2.556$ Å.

## III. SINGLE-PARTICLE MODEL

In this section we limit ourselves to a special class of variational wave functions which have many of the basic properties of the true wave function provided the assumptions in Sec. II are valid. From this class we show how to obtain that $\Psi(V)$ which gives the lowest calculated energy for each $V$, i.e., we obtain the best $\tilde{U}_0(V)$ as a function of $V$. We then calculate $\tilde{\mathcal{H}}_0(P)$ to obtain the lowest upper bound for the ground-state enthalpy of the system under pressure $P$.

Taking into account thoughts of simplicity as well as the basic assumptions, we choose initially as our generic many-body wave function

$$\Psi_P\equiv\sum_P P\prod_{i=1}^{N}\psi_i(\mathbf{r}_i)\eta_i(\xi_i), \tag{3.1}$$

where

$$\sum_P P$$

is the permutation operator for Fermi statistics, and the spin function $\eta_i(\xi_i)$ describes particle $i$ in spin-state $\eta_i$.

Now, because $v_{LJ}(r)$ is strongly repulsive at small distances, we expect each $\psi_i$ to be rigorously confined to a single-lattice cell. We therefore postulate (and verify self-consistently later) that our $\psi_i$ are of the Heitler-London type and have zero overlap, so that

$$\int\psi_i(\mathbf{r})\psi_j(\mathbf{r})d\mathbf{r}=0, \quad i\neq j. \tag{3.2}$$

Because of this zero overlap, it is clear that

$$\langle\Psi_P|H|\Psi_P\rangle=\langle\Psi|H|\Psi\rangle, \tag{3.3}$$

where $H$ is the Hamiltonian given in Eq. (2.1), and

$$\Psi\equiv\prod_{i=1}^{N}\psi_i(\mathbf{r}_i). \tag{3.4}$$

Since the simpler generic wavefunction $\Psi$ gives the same energy as the more complicated $\Psi_P$, we use it instead of $\Psi_P$.

Because of the spatial symmetry of the crystal, and for reasons of simplicity, we postulate that each $\psi_i$ has the same functional form relative to its own lattice site, i.e.,

$$\psi_i(\mathbf{r}_i)=\psi(\mathbf{r}_i-\mathbf{R}_i), \tag{3.5}$$

where $\mathbf{R}_i$ is the position of the $i$th lattice site, and, for convenience, we choose lattice site 1 to be at the origin of our configuration space coordinates, i.e., $\mathbf{R}_1=0$. [From Eq. (3.5) it is clear that the wave function $\Psi$ is a function of the volume since the $\psi_i$ are functions of

$\mathbf{R}_i$, and these lattice site positions are, of course, functions of the volume.]

Because of the cubic symmetry of the crystal, we would like $\psi$ to be cubically symmetric and, in particular, we may choose it to have the form

$$\psi(\mathbf{r})=u_0(r)+u_4(r)K_4(\Omega), \tag{3.6}$$

where $K_4(\Omega)$ is the Kubic harmonic of the $\alpha$ type (identity representation) with angular momentum $l=4$; $u_0(r)$ and $u_4(r)$ are arbitrary functions of $r$. [These Kubic harmonics (KH) were introduced by Von der Lage and Bethe[7] in 1947. In Appendix A we give a table of the $\alpha$ type KH up to $l=8$, state their basic properties, and explain our motivation for choosing these $\alpha$ type KH.] The wave function shown in Eq. (3.6) satisfies

$$\langle\psi(\mathbf{r})|K_l(\Omega)\rangle=0, \quad l\geq 6, \tag{3.7}$$

and it will be seen to be convenient to use Eq. (3.7), which is less stringent than Eq. (3.6), as our constraint.

We normalize our wave functions,

$$\langle\psi(\mathbf{r})|\psi(\mathbf{r})\rangle=1, \tag{3.8}$$

and, in order to simplify the manipulations, we further assume that $\Psi$ is real. Our problem then becomes, in the language of the calculus of variations, to solve

$$\delta E\equiv\delta\langle\prod_{i=1}^{N}\psi_i|H|\prod_{i=1}^{N}\psi_i\rangle=0, \tag{3.9}$$

subject to the constraints

$$\text{(a)}\quad \psi_i=\psi(\mathbf{r}_i-\mathbf{R}_i), \tag{3.10a}$$

$$\text{(b)}\quad \langle\psi(\mathbf{r})|K_l(\Omega)\rangle=0, \quad l\geq 6, \tag{3.10b}$$

$$\text{(c)}\quad \langle\psi(\mathbf{r})|\psi(\mathbf{r})\rangle=1. \tag{3.10c}$$

The constraints imply that

$$\langle\delta\psi(\mathbf{r})|K_l(\Omega)\rangle=0, \quad l\geq 6, \tag{3.11}$$

and

$$\langle\delta\psi(\mathbf{r})|\psi(\mathbf{r})\rangle=0; \tag{3.12}$$

from which it follows in a straightforward fashion that a sufficient condition for Eq. (3.9) to be satisfied is that $\psi(\mathbf{r})$ satisfies, in addition to the constraints (3.10), the equation

$$[(-\hbar^2/2m)\nabla^2+W(\mathbf{r})]\psi(\mathbf{r}) = \epsilon\psi(\mathbf{r})+\sum_{l=6}^{K}\beta_l(r)K_l(\Omega), \tag{3.13}$$

where $W(\mathbf{r})$ is the Hartree potential given by

$$W(\mathbf{r}_1)=\sum_{j\neq 1}\int[\psi(\mathbf{r}_2-\mathbf{R}_j)]^2 v_{LJ}(r_{12})d\mathbf{r}_2; \tag{3.14}$$

$\epsilon$ is the single-particle energy eigenvalue, and $\beta_l(r)$ is an arbitrary function of $r$ to be determined later.

$$\sum_{l=6}^{K}$$

means that the sum includes only those $l$ for which there exist Kubic harmonics of the $\alpha$ type starting from $l=6$. It is also easily shown that

$$E=N[\epsilon-\tfrac{1}{2}W], \tag{3.15}$$

where

$$W\equiv\langle\psi(\mathbf{r})|W(\mathbf{r})|\psi(\mathbf{r})\rangle. \tag{3.16}$$

Note that Eq. (3.13), for various values of $\epsilon$ and $\beta_l(r)$, will be valid for any local minimum of the energy, i.e., for excited energy eigenstates as well as for the ground state of the system. To obtain the ground state, we see from Eq. (3.15) that the energy does not depend explicitly on the functions $\beta_l(r)$, and is a minimum when $\epsilon$ is a minimum. Hence, when solving Eq. (3.13) we seek the lowest possible eigenvalue, $\epsilon_0$, and then the lowest calculated energy state for the system is

$$\tilde{U}_0=N[\epsilon_0-\tfrac{1}{2}W]. \tag{3.17}$$

The choice of the functions $\beta_l(r)$ will be explained subsequently. In the usual derivation of the spherically symmetric Hartree equations,[8] the constraints (3.10b) are not used, and hence the $\beta_l(r)$ do not appear. It will, however, be manifest in the following that, whenever dealing with a cubic lattice, self-consistency demands the use of these $\beta_l(r)$.

We now proceed to show that, by using a self-consistent iteration procedure, a solution of Eq. (3.13) can be found which satisfies the constraints (3.10). In particular, we will exhibit a solution of the form

$$\psi(\mathbf{r})=u_0(r)+u_4(r)K_4(\Omega), \tag{3.18a}$$

$$\langle\psi(\mathbf{r})|\psi(\mathbf{r})\rangle=1. \tag{3.18b}$$

To start the iteration procedure, let us guess at some initial wave function which satisfies Eqs. (3.18), and then consider the sum formed using this wavefunction,

$$S(\mathbf{r})=\sum_{j\neq 1}[\psi(\mathbf{r}-\mathbf{R}_j)]^2. \tag{3.19}$$

Recalling the properties of the KH given in Appendix A, it is straightforward to show that $S(\mathbf{r})$ remains invariant under all cubic-symmetry operations so that we may expand $S(\mathbf{r}_2)$ in the form

$$\sum_{j\neq 1}[\psi(\mathbf{r}_2-\mathbf{R}_j)]^2=\sum_{n=0}^{K}S_n(r_2)K_n(\Omega_2), \tag{3.20}$$

where

$$S_n(r)=\frac{1}{4\pi}\sum_{j\neq 1}\int[\psi(\mathbf{r}-\mathbf{R}_j)]^2K_n(\Omega)d\Omega. \tag{3.21}$$

[7] F. C. Von der Lage and H. A. Bethe, Phys. Rev. **71**, 612 (1947).

[8] F. Seitz, *Modern Theory of Solids* (McGraw-Hill Book Company, Inc., New York, 1960).

We also expand $v_{LJ}(r)$:

$$v_{LJ}(r_{12})=\sum_{l=0}^{\infty} J_l(r_1,r_2)P_l(\cos\gamma_{12}), \tag{3.22}$$

where

$$J_l(r_1,r_2)=\tfrac{1}{2}(2l+1)\int_{-1}^{1} v_{LJ}(r_{12})P_l(\cos\gamma_{12}) \times d(\cos\gamma_{12}). \tag{3.23}$$

We then use the addition theorem for Legendre polynomials on $P_l(\cos\gamma_{12})$, and putting Eqs. (3.20) and (3.22) into Eq. (3.14), recalling the well-known orthogonality conditions on the transcendental functions and on the Legendre polynomials, we obtain at once

$$W(\mathbf{r})=\sum_{n=0}^{K} W_n(r)K_n(\Omega), \tag{3.24}$$

where

$$W_n(r_1)=\frac{4\pi}{2n+1}\int S_n(r_2)J_n(r_1,r_2)r_2^2dr_2. \tag{3.25}$$

To obtain the expansion (3.24), we used only the following three properties: (a) All the $\psi_i$ have the same functional form about their respective lattice sites, (b) $\psi(\mathbf{r})$ remains invariant under all cubic symmetry operations, and (c) the sum

$$\sum_{j\neq 1}$$

was taken over a cubic lattice. In particular, it should be noted that we would have obtained the same expansion (3.24) even if we had taken $\psi(\mathbf{r})$ to be only spherically symmetric.

Using Eq. (3.24), our problem now is to show that there exists a solution $\psi(\mathbf{r})$ of the equation

$$[(-\hbar^2/2m)\nabla^2+\sum_{n=0}^{K} W_n(r)K_n(\Omega)-\epsilon]\psi(\mathbf{r}) =\sum_{l=6}^{K}\beta_l(r)K_l(\Omega), \tag{3.26}$$

which satisfies Eqs. (3.18). For our present purposes, the $W_n(r)$ in Eq. (3.26) are taken to be any given real functions of $r$, and we ignore the fact that they are actually functions of $\psi$. Define

$$u_0(r)\equiv s(r)/r, \tag{3.27a}$$

$$u_4(r)\equiv g(r)/r. \tag{3.27b}$$

Using the properties of the KH, and the well-known fact that

$$\left[\frac{1}{\sin\theta}\frac{\partial}{\partial\theta}\left(\sin\theta\frac{\partial}{\partial\theta}\right)+\frac{1}{\sin^2\theta}\frac{\partial^2}{\partial\varphi^2}\right]Y_{lm}(\theta,\varphi) =-l(l+1)Y_{lm}(\theta,\varphi), \tag{3.28}$$

we obtain for the kinetic energy term

$$(-\hbar^2/2m)\nabla^2\psi(r) =\left[\frac{-\hbar^2}{2m}\right]\left[\frac{1}{r}\right]\left[\frac{d^2s}{dr^2}+K_4(\Omega)\left(\frac{d^2g}{dr^2}-\frac{20g}{r^2}\right)\right]. \tag{3.29}$$

Before proceeding to the potential energy, we note first that the product $K_4(\Omega)K_j(\Omega)$ remains invariant under all cubic symmetry operations so that we may write

$$K_4(\Omega)K_j(\Omega)=\sum_{k=0}^{K} D_{jk}K_k(\Omega), \tag{3.30}$$

where

$$D_{jk}=\frac{1}{4\pi}\int K_j(\Omega)K_k(\Omega)K_4(\Omega)d\Omega. \tag{3.31}$$

(From the rules for the addition of angular momenta, it is clear that $D_{jk}\neq 0$ only if $j,k$ satisfy $|j-4|\leq k\leq j+4$.) The potential energy term is then

$$[\sum_{n=0}^{K} W_n(r)K_n(\Omega)][u_0(r)+u_4(r)K_4(\Omega)] =\sum_{n=0}^{K} K_n(\Omega)[u_0(r)W_n(r)+u_4(r)\sum_{k=0}^{K} D_{kn}W_k(r)]. \tag{3.32}$$

Putting Eqs. (3.29) and (3.32) into Eq. (3.26) and recalling the orthogonality of the KH, we see that the necessary and sufficient conditions for Eq. (3.26) to be satisfied are that we set

$$\beta_l(r)=u_0(r)W_l(r)+u_4(r)\sum_{k=0}^{K} D_{kl}W_k(r), \quad l\geq 6, \tag{3.33}$$

and that $s(r)$ and $g(r)$ satisfy the coupled set of equations

$$\left(\frac{-\hbar^2}{2m}\right)\left(\frac{d^2s(r)}{dr^2}\right)+W_0(r)s(r)+W_4(r)g(r) -\epsilon s(r)=0, \tag{3.34a}$$

$$\left(\frac{-\hbar^2}{2m}\right)\left(\frac{d^2g(r)}{dr^2}\right)+B(r)g(r)+W_4(r)s(r) -\epsilon g(r)=0, \tag{3.34b}$$

where

$$B(r)\equiv\left(\frac{-\hbar^2}{2m}\right)\frac{20}{r^2}+W_0(r)+0.577W_4(r) +0.713W_6(r)+0.682W_8(r). \tag{3.35}$$

In the above we have used

$$D_{04}=D_{40}=1, \tag{3.36a}$$

$$D_{44}=0.577, \tag{3.36b}$$

$$D_{64}=0.713, \tag{3.36c}$$

and

$$D_{84}=0.682. \tag{3.36d}$$

Note further that if $[s(r),g(r)]$ satisfies the coupled set of equations (3.34) so does $[Cs(r),Cg(r)]$ where $C$ is any constant. We choose $C$ to be such that our wave function [Eq. (3.18a)] is normalized to one, i.e.,

$$C^{-2}=4\pi\left(\int s^2dr+\int g^2dr\right). \tag{3.37}$$

We have thus shown that if we use any initial wave function which satisfies Eqs. (3.18) to calculate the Hartree potential $W(\mathbf{r})$, then Eq. (3.13) may be written in the form (3.26) and we get back a solution which satisfies Eqs. (3.18). This then serves as the basis for an iterative self-consistent solution of Eq. (3.13) subject to the constraints (3.10).

For convenience, we now summarize the calculational procedure to be followed. The details of the numerical methods used are given in Appendix B.

(a) Calculate $J_l(r_1,r_2)$ using Eq. (3.23) for $l=0$, 4, 6, 8. (b) Choose an initial $\psi(\mathbf{r})$ which satisfies Eqs. (3.18). (c) Calculate $S_l(r)$ using Eq. (3.21) for $l=0$, 4, 6, 8. (d) Calculate $W_l(r)$ using Eq. (3.25) for $l=0$, 4, 6, 8. (e) Solve the coupled set of equations (3.34) for $\epsilon$ and $[s(r),g(r)]$. In this solution we seek the lowest possible $\epsilon$. (f) Normalize the wave function $\psi(\mathbf{r})$. That is, use $[Cs(r),Cg(r)]$ where $C$ is given by Eq. (3.37). Then

$$\tilde{U}_0=N[\epsilon_0-\tfrac{1}{2}W], \tag{3.38}$$

where

$$W=4\pi\int[W_0s^2+2sgW_4 +g^2(W_0+0.577W_4+0.713W_6+0.682W_8)]dr. \tag{3.39}$$

We now use $[Cs(r),Cg(r)]$ to replace the initial choice given in step (b), and repeat the subsequent steps. Repeating this procedure several times, we obtain a (hopefully) convergent set of minimum energies

$$\tilde{U}_0^{(1)},\quad \tilde{U}_0^{(2)},\quad \tilde{U}_0^{(3)},\quad \cdots, \tag{3.40}$$

where the superscripts refer to iteration numbers. When

$$|\tilde{U}_0^{(i-1)}-\tilde{U}_0^{(i)}|/|\tilde{U}_0^{(i)}|$$

is small enough to insure an accuracy of better than 1%, we stop the procedure and take the last obtained $\tilde{U}_0$ as our calculated ground-state energy.

The magnitudes of the lattice-site positions are expressible as multiples of the nearest-neighbor distance $A$, and thus by varying $A$ we are able to obtain $\tilde{U}_0$ as a function of the volume. We plot $\tilde{U}_0(V)$ versus $V$ and, using Eq. (2.4), we determine $\tilde{V}_g$ corresponding to the experimentally observed pressure $P_g$. We then obtain the lowest calculated upper bound to the enthalpy, viz.,

$$\tilde{\mathcal{H}}_0(P_g)=\tilde{U}_0(\tilde{V}_g)+P_g\tilde{V}_g. \tag{3.41}$$

The results obtained by applying the methods of this section to solid $He^3$ at 0°K are given in Sec. IV.

One obvious point should be mentioned before proceeding. If we wish to find a rigorous upper bound for the energy using only spherically symmetric single-particle wave functions, we must explicitly use the constraint

$$\langle\psi(\mathbf{r})|K_l(\Omega)\rangle=0,\quad \text{all}\quad l\neq 0, \tag{3.42}$$

instead of constraint (3.10b), at the start of the problem. For, as shown above, the Hartree potential for a cubic lattice is cubically symmetric even if the wave functions are taken to be only spherically symmetric, and the constraints (3.42) are necessary to supply sufficient $\beta_l(r)$ functions to cancel out the "unwanted" terms in the infinite expansion of the Hartree potential. We may then obtain the spherically symmetric self-consistent solution

$$\psi(r)=s(r)/r, \tag{3.43}$$

where $s(r)$ satisfies the equation

$$\left(-\frac{\hbar^2}{2m}\right)\frac{d^2s}{dr^2}+W_0(r)s(r)-\epsilon s(r)=0, \tag{3.44}$$

where $W_0(r)$ is defined by Eq. (3.25) with $n=0$. Equation (3.44) was solved numerically for solid $He^3$ by Nosanow and Shaw.[5] Because of the simplicity with which our computer programs can be adapted to this case, we will repeat it as a comparison base for the cubically symmetric calculation and as a rough check on the computer programs we use.

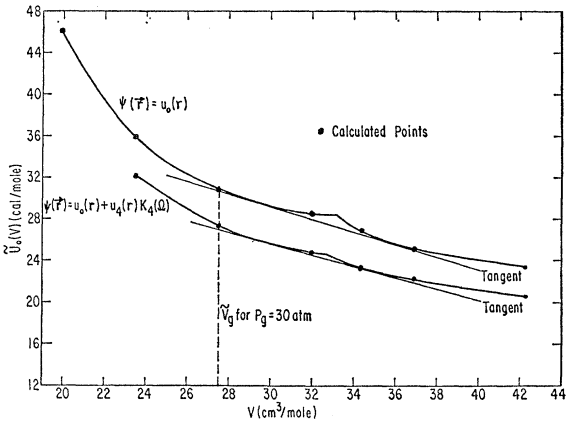


FIG. 2. Calculated ground-state energy of solid $He^3$ as a function of volume, using the Lennard-Jones two-body potential. The top curve was obtained by using spherically symmetric single-particle wave functions, and the bottom one was obtained by using cubically symmetric single-particle wave functions of the form $\psi(\mathbf{r})=u_0(r)+u_4(r)K_4(\Omega)$ and the Hartree potential $W(\mathbf{r})=W_0(r)+W_4(r)K_4(\Omega)$, as explained in Sec. IVB.

## IV. RESULTS AND DISCUSSION

The results of our calculations are given in Table I and Figs. 2 to 5 inclusively. The numerical computa-

TABLE I. Values of the enthalpy ($\mathcal{H}_0$), the ground-state energy ($U_0$), and the volume ($V$) for solid $He^3$ under a pressure of 30 atm at $T=0$°K. $C$ refers to cubically symmetric single-particle wave functions and $S$ to spherically symmetric ones. Both calculations were done using the Lennard-Jones two-body potential. See remarks on the experimental value in Sec. IV.

| | $V$(cm³/mole) | $U_0$(cal/mole) | $\mathcal{H}_0$(cal/mole) |
|---|---|---|---|
| Calculation $S$ | 27.5 | 30.8 | 50.8 |
| Calculation $C$ | 27.5 | 27.3 | 47.3 |
| Experiment | 24.9 | −1.6 | 16.5 |

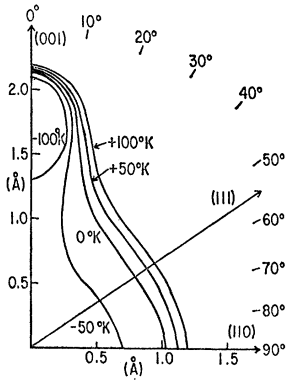


FIG. 3. Contour plot of the Hartree potential $W(\mathbf{r})=W_0(r)+W_4(r)K_4(\Omega)$ for solid $He^3$ at a fixed volume of 23.49 $cm^3$/mole using cubically symmetric single-particle wave functions and the Lennard-Jones two-body potential. The minimum calculated single-particle energy is $\epsilon_0=-5.8°K$, and the calculated ground-state energy for this case is 32.1 cal/mole. The above plot is in the $\varphi=45°$ plane.

tions were carried out on the CDC 3600 digital computer at the University of California, San Diego.

Since the self-consistent equations are nonlinear, there is always the possibility of more than one solution. All the solutions we show were obtained by using as the starting wave function for our iteration sequence the Gaussian

$$\begin{aligned}\psi_{\text{start}}(r)&=C\exp(-r^2), \quad r<\tfrac{1}{2}A\\ \psi_{\text{start}}(r)&=0, \quad r\geq\tfrac{1}{2}A\end{aligned} \tag{4.1}$$

where $A$ is the nearest-neighbor distance, and $C$ is a constant such that $\psi(r)$ is normalized to one.

In the following discussions, we review first the known experimental data, and then we give the results of our calculations using the $LJ$ potential.

### A. Experimental Results

In order to calculate the experimental value of the internal energy of solid $He^3$ at 0°K, we use the following data from the review article by Bernardes and Brewer[2]: The extrapolated latent heat of evaporation of liquid $He^3$ at 0°K is $L_0=5.0$ cal/mole. The liquid solidifies at 0°K under an external pressure of 30 atm, and at this pressure and temperature, the volume of the liquid is 26 $cm^3$/mole, and that of the solid is 24.9 $cm^3$/mole.

Since $L_0=5.0$ cal/mole, the internal energy of liquid $He^3$ at zero temperature and pressure is $-5.0$ cal/mole. The increase in the internal energy of the liquid upon the application of 30 atm pressure can be calculated from the integral $-\int PdV$, which gives 2.6 cal/mole using the data of Sherman and Edeskuty[9] for the liquid at 1.6°K (and assuming them to be approximately valid at 0°K). Finally, we have to calculate the internal energy difference between the liquid and solid under 30 atm pressure at 0°K. We have

$$\Delta U=\rho-P\Delta V, \tag{4.2}$$

where $\rho$ is the latent heat of melting. Now, using the Clausius-Clapeyron equation,

$$\rho=T\Delta V(dP/dT), \tag{4.3}$$

and since $\Delta V$ is finite, we have at $T=0°K$ that $\rho=0$.

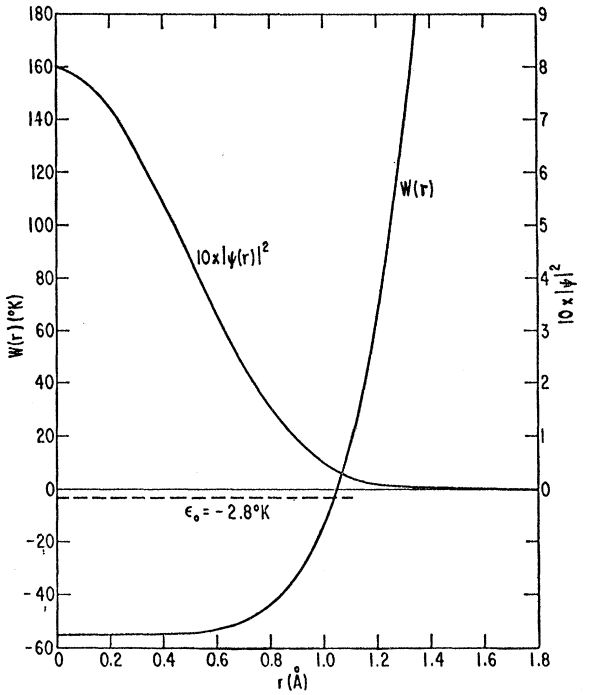


FIG. 5. Results of the Hartree calculation for the ground state of solid $He^3$ at a fixed volume of 23.49 $cm^3$/mole, using spherically symmetric single-particle wave functions and the Lennard-Jones two-body potential. $|\psi(r)|^2$ is the square of the normalized spherically symmetric single-particle wave function, and $W(r)\equiv W_0(r)$ is the Hartree potential used in the calculation. The minimum calculated single-particle energy is $\epsilon_0=-2.8°K$ and the calculated ground-state energy for this case is 35.9 cal/mole.

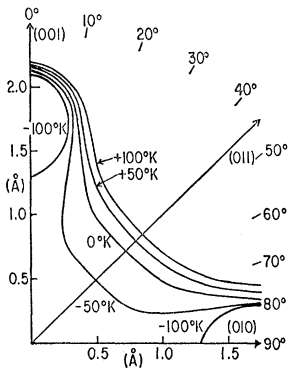


FIG. 4. As Fig. 3, but in the $\varphi=90°$ plane.

Then, using $P=30$ atm and $\Delta V=1.1$ $cm^3$/mole, we get from Eq. (4.2) that $\Delta U=0.8$ cal/mole. Adding up all the contributions, we then obtain that the experimental internal energy of solid $He^3$ at 0°K is $(-1.6)$ cal/mole.

It must be emphasized that this experimental result is dependent upon several assumptions, not all of which are firmly established. In particular, since the melting

[9] R. H. Sherman and F. J. Edeskuty, Ann. Phys. (N. Y.) 9, 522 (1960).

curve for $He^3$ exhibits a minimum at 0.3°K, it is very difficult to extrapolate and find the melting pressure at 0°K with any confidence. The choice of 30 atm at 0°K could therefore be wrong by as much as 10 atm or more.

### B. Single-Particle Model

First, we see in Table I that an improvement of only 8% is obtained in the calculated enthalpy (at 30 atm and 0°K) by using cubically symmetric single-particle wave functions instead of spherically symmetric ones, and this despite the fact that the cubically symmetric Hartree potential differs significantly from sphericity (Figs. 3 and 4). The best calculated enthalpy (47.3 cal/mole) is still significantly higher than the probable experimental value (16.5 cal/mole).

It is seen explicitly in Fig. 5 that $W(r)\to\infty$ as $r\to(\frac{1}{2}A)$ so that rigorously preventing our single-particle wave functions from overlapping leads to completely self-consistent results.

The "change of phase" which both the energy curves exhibit (Fig. 2) occurs at approximately 25 atm. Its significance is not completely clear since a fixed crystal structure was imposed upon the calculation for each of the plotted points.

At a volume of 23.49 $cm^3$/mole ($A=3.7$ Å), the complete calculation was carried out using the four potentials $W_0(r)$, $W_4(r)$, $W_6(r)$, $W_8(r)$, and, for comparison, the calculation was repeated using only the two potentials $W_0(r)$, $W_4(r)$, and setting $W_6(r)=W_8(r)=0$, all $r$. The results of both calculations were the same to three figures of accuracy so that subsequently only the two potentials $W_0(r)$, $W_4(r)$ were used, it being assumed that $W_6(r)$, $W_8(r)$ always have negligible effect in comparison. Certain numerical approximations were also made during the course of the calculations and these are described in detail in Appendix B. The calculated volumes shown in Table I were obtained by plotting $[\tilde{U}_0(V)+PV]$ versus $V$ for $P=30$ atm, and then finding that $V$ at which the minimum occurred. Because of unavoidable inaccuracies in plotting, these values may be in error by as much as 0.5 $cm^3$/mole. The energy and enthalpy values are considered to be accurate to within 0.1 cal/mole.

It is instructive to compare our results with the classical enthalpy of a crystal with the same external conditions imposed on it as were imposed on our quantum-mechanical calculation, i.e., we wish to compare our results with the classical enthalpy of a bcc crystal under 30 atm pressure. This value is roughly obtained by considering the atoms to have no kinetic energy, and (at 30 atm) to be rigidly spaced at a nearest-neighbor distance of about 2.8 Å (just above the bottom of the $LJ$ well). We then see that the classical enthalpy is of the order of $-80$ cal/mole. Hence, the difference between the experimental and classical values of the enthalpy (the "quantum effect") is of the order of 100 cal/mole. The difference between our calculated value and the experimental value is thus 30% of the quantum effect, and this is to be attributed to the fact that we did not include either exchange or correlation effects in the calculations.


## ACKNOWLEDGMENTS

The author is most grateful to Professor Keith A. Brueckner for suggesting this problem and for his constant encouragement and advice, and to Dr. Katuro Sawada for many constructive criticisms and illuminating discussions. He also wishes to thank Professor Clay Perry, Director of the Computer Center at the University of California, San Diego, for the full cooperation of his organization, and Mrs. Anna J. Devore for much helpful advice on computer programming.


## APPENDIX A. KUBIC HARMONICS

Von der Lage and Bethe[7] have shown how to construct wave functions whose group is the full cubic symmetry group. These wave functions, which they named Kubic harmonics (KH), fall into 10 irreducible representations (types). In this Appendix we state some of the important properties of the $\alpha$-type KH (identity representation), and then explain our motivation for choosing this representation.

### Properties of the Kubic Harmonics

The eight $\alpha$ type KH which we have occasion to use are

$$K_0=1, \tag{A1}$$

$$K_4=\frac{5\times(3\times7)^{1/2}}{4}\left[\frac{x^4+y^4+z^4}{r^4}-\frac{3}{5}\right], \tag{A2}$$

$$K_6=\frac{3\times7\times11\times(2\times13)^{1/2}}{8}\left[\frac{x^2y^2z^2}{r^6}+\frac{1}{22}[K_4]-\frac{1}{105}\right], \tag{A3}$$

$$K_8=\frac{5\times13\times(3\times11\times17)^{1/2}}{16}\left[\frac{x^8+y^8+z^8}{r^8}-\frac{28}{5}[K_6]-\frac{210}{143}[K_4]-\frac{1}{3}\right], \tag{A4}$$

where functions in square brackets indicate functions with normalization factors omitted. ($K_8$ as given in Ref. 8 is erroneous.)

Any of the $\alpha$ type KH can be written in the form

$$K_l(\Omega)=\sum_{m=-l}^{l} C_{lm}Y_{lm}(\theta,\varphi), \tag{A5}$$

or

$$K_l(\Omega)=\sum_{m=0}^{l}(A_{lm}\cos m\varphi+B_{lm}\sin m\varphi)P_{lm}(\cos\theta), \quad \text{(A6)}$$

where $Y_{lm}(\theta,\varphi)$ and $P_{lm}(\cos\theta)$ are the usual spherical harmonics and Legendre polynomials, respectively, and $A_{lm}$, $B_{lm}$, $C_{lm}$ are constants, some of which may be zero. The KH are normalized to $4\pi$.

Being the identity representation means, of course, that the $\alpha$ type KH remain invariant under all 48 cubic symmetry operations. Moreover, from their mode of construction[7] it is clear that the $\alpha$-type KH span the space of all well-behaved functions of the angles $\theta$ and $\varphi$ which remain invariant under all cubic symmetry operations. That is, if $f(\mathbf{r})$ is a well-behaved function of $\mathbf{r}$ such that

$$f(\mathfrak{R}^{-1}\mathbf{r})=f(\mathbf{r}), \quad \text{(A7)}$$

for all cubic symmetry operations $\mathfrak{R}$, then $f(\mathbf{r})$ may always be expanded in the form

$$f(\mathbf{r})=\sum_{l=0}^{K} g_l(r)K_l(\Omega), \quad \text{(A8)}$$

where

$$g_l(r)=\frac{1}{4\pi}\int f(\mathbf{r})K_l(\Omega)d\Omega. \quad \text{(A9)}$$

### Choice of Irreducible Representation

It is well known that irreducible representations generally do not mix so that, if we pick one part of our wave function to be of the $\alpha$ type, we must continue with this type for the remainder. The irreducible representation member $K_0=1$ is desirable since it has no nodes, and therefore $u_0(r)+u_4(r)K_4(\Omega)$ may also turn out to have no nodes which is the usual situation for the ground-state wave function of any given system. This choice has the additional advantage that one of the limits of the wave function is the spherically symmetric case, thus facilitating comparison with previous work. Also, the $\alpha$ type KH are nondegenerate which is again typical of ground-state wave functions. Finally, (and perhaps above all) *a posteriori*, we see that the wave function $\psi(\mathbf{r})=u_0(r)+u_4(r)K_4(\Omega)$ leads most simply and directly to self-consistent results.

## APPENDIX B. NUMERICAL METHODS

### Calculation of $J_l(r_1,r_2)$

For the *LJ* two-body potential we have

$$J_l(r_1,r_2)=\frac{1}{2}\int 4\epsilon\left[\frac{\sigma^{12}}{(a+b\mu)^6}-\frac{\sigma^6}{(a+b\mu)^3}\right]P_{l0}(\mu)d\mu, \quad \text{(B1)}$$

where

$$a\equiv r_1^2+r_2^2; \quad b\equiv -2r_1r_2. \quad \text{(B2)}$$

Now for convenience on the computer, we use in actual fact as our two-body potential in all the calculations

$$\begin{aligned} v(r)&=v_{LJ}(r), \quad r>1.60\ \text{Å},\\ v(r)&=10^4\ ^\circ\text{K}, \quad r\leq 1.60\ \text{Å}. \end{aligned} \quad \text{(B3)}$$

Noting that $P_{l0}(\mu)$ is a polynomial of powers of $\mu$, it is clear that the integral (B1) can be done explicitly by using the transformation $y\rightarrow a+b\mu$,

$$\int\frac{\mu^n}{(a+b\mu)^6}d\mu\rightarrow\frac{1}{b^{n+1}}\int\frac{(y-a)^n}{y^6}dy. \quad \text{(B4)}$$

However, if $a$ is large and $b$ is small, this will give very poor numerical accuracy since, in evaluating $P_{l0}(\mu)$ (especially for $l=8$) we will be dealing with very small differences between large numbers, such that we would have to use double-precision computer accuracy to obtain meaningful results. Hence, in the case $a\gg b$, we use $x=b\mu/a$ as an expansion parameter and obtain, for example,

$$\int\frac{\mu^n}{(a+b\mu)^6}d\mu=\frac{a^{n+1}}{a^6b^{n+1}}\int\frac{x^n}{(1+x)^6}dx. \quad \text{(B5)}$$

Then, expanding the denominator and integrating, we get

$$\int\frac{\mu^n}{(a+b\mu)^6}d\mu=\frac{\mu^{n+1}}{a^6}\left[\frac{1}{n+1}-\frac{6x}{n+2}+\frac{6(6+1)x^2}{2!(n+3)}-\cdots\right]. \quad \text{(B6)}$$

The sum in square brackets is continued until terms are so small as not to affect the final result to within our desired accuracy (typically until we reach terms which are $10^{-7}$ of the leading term).

Using the above methods we calculate and store on tape the functions $J_l(r_1,r_2)$ for all values of $r_1$ and $r_2$ which will subsequently be needed in steps of $h=0.05$ Å.

### Calculation of $S_l(r)$ and $W_l(r)$

We first define the coordinate notation to be used in the following: $\mathbf{R}_i$ is the position of the $i$th lattice site, and, for convenience, lattice site 1 is chosen to be at the origin of the configuration space coordinates, i.e., $\mathbf{R}_1=0$. A set of parallel Cartesian coordinate systems are assumed to be affixed one at each lattice site. $\mathbf{r}_j^{(i)}$ is then the position of the $j$th particle (subscript) relative to the coordinate system at lattice site $i$ (superscript). A similar notation is used for the angles. Both the subscript and superscript 1 will be suppressed when convenient.

Define

$$S_l(j,r)\equiv\frac{1}{4\pi}\int[\psi(\mathbf{r}-\mathbf{R}_j)]^2K_l(\Omega)d\Omega. \quad \text{(B7)}$$

Let our lattice sites be so numbered that the sites $j=2$ to $j=9$, inclusively, refer to the nearest neighbors to site No. 1, and let lattice site No. 2 be at $(\frac{1}{2},\frac{1}{2},\frac{1}{2})$.

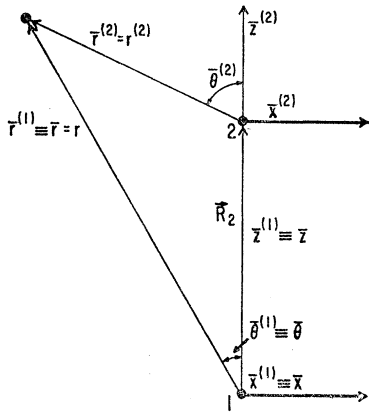


FIG. 6. Coordinate notation after rotation so that $z\rightarrow\bar{z}$ where $\bar{z}$ and $\mathbf{R}_2$ are collinear.

Consider now $S_l(2,r)$. The coordinates centered at lattice site No. 1 are rotated so that $z\rightarrow\bar{z}$ where $\bar{z}$ and $\mathbf{R}_2$ are collinear, and, similarly, the coordinates centered at site No. 2 are rotated so that they remain parallel to those centered at site No. 1. Putting in the proper values for the transcendental functions in the transposed rotation matrix,[10] we may then write

$$\begin{bmatrix} x^{(i)} \\ y^{(i)} \\ z^{(i)} \end{bmatrix} = \begin{bmatrix} -1/\sqrt{2} & -1/\sqrt{6} & 1/\sqrt{3} \\ 1/\sqrt{2} & -1/\sqrt{6} & 1/\sqrt{3} \\ 0 & \sqrt{2}/\sqrt{3} & 1/\sqrt{3} \end{bmatrix} \begin{bmatrix} \bar{x}^{(i)} \\ \bar{y}^{(i)} \\ \bar{z}^{(i)} \end{bmatrix}, \quad i=1,2, \tag{B8}$$

from which, for all $l$,

$$K_l(\theta^{(i)},\varphi^{(i)})=\bar{K}_l(\bar{\theta}^{(i)},\bar{\varphi}^{(i)}), \quad i=1,2, \tag{B9}$$

where $\bar{K}_l$ indicates a change of functional form from $K_l$. The new coordinate system is shown in Fig. 6, and it is seen at once that

$$(r^{(2)})^2=(r^{(1)})^2+(R_2)^2-2r^{(1)}R_2\cos\bar{\theta}^{(1)}, \tag{B10}$$

from which it follows by differentiation that

$$\sin\bar{\theta}^{(1)}d\bar{\theta}^{(1)}=\frac{r^{(2)}dr^{(2)}}{r^{(1)}R_2}. \tag{B11}$$

The value of the determinant of the rotation matrix is one, and this is the Jacobian for the transformation so that

$$d\Omega\rightarrow d\bar{\Omega}\equiv\sin\bar{\theta}^{(1)}d\bar{\theta}^{(1)}d\bar{\varphi}^{(1)}=\frac{r^{(2)}dr^{(2)}d\bar{\varphi}^{(1)}}{r^{(1)}R_2}, \tag{B12}$$

and

$$S_l(2,r)=\frac{1}{4\pi}\int\left[\frac{s(r^{(2)})+g(r^{(2)})\bar{K}_4(\bar{\theta}^{(2)},\bar{\varphi})}{r^{(2)}}\right]^2 \times\bar{K}_l(\bar{\theta},\bar{\varphi})\frac{r^{(2)}dr^{(2)}d\bar{\varphi}}{rR_2}, \tag{B13}$$

where we have used the fact that in the new coordinate systems (unlike the case before rotation),

$$\bar{\varphi}^{(2)}=\bar{\varphi}^{(1)}\equiv\bar{\varphi}. \tag{B14}$$

From Fig. 6 we note that

$$r\cos\bar{\theta}=R_2+r^{(2)}\cos\bar{\theta}^{(2)}, \tag{B15}$$

so that

$$\cos\bar{\theta}^{(2)}=\frac{r\cos\bar{\theta}}{r^{(2)}}-\frac{R_2}{r^{(2)}}, \tag{B16}$$

and from Eq. (B10) we have

$$\cos\bar{\theta}=\frac{(r)^2+(R_2)^2-(r^{(2)})^2}{2rR_2}, \tag{B17}$$

i.e., both $\bar{\theta}$ and $\bar{\theta}^{(2)}$ may be expressed in terms of $r$, $R_2$, and $r^{(2)}$, so that we may define

$$I_l^{(a)}(r,r^{(2)},R_2)=\frac{1}{2\pi}\int\bar{K}_l(\bar{\theta},\bar{\varphi})d\bar{\varphi}, \tag{B18a}$$

$$I_l^{(b)}(r,r^{(2)},R_2)=\frac{1}{2\pi}\int\bar{K}_4(\bar{\theta}^{(2)},\bar{\varphi})\bar{K}_l(\bar{\theta},\bar{\varphi})d\bar{\varphi}, \tag{B18b}$$

$$I_l^{(c)}(r,r^{(2)},R_2)=\frac{1}{2\pi}\int[\bar{K}_4(\bar{\theta}^{(2)},\bar{\varphi})]^2[\bar{K}_l(\bar{\theta},\bar{\varphi})]d\bar{\varphi}. \tag{B18c}$$

Since the $I_l$'s above are independent of the wave functions, they need only be calculated (numerically) once for those values of the parameters which are subsequently needed, and they are then stored on tape for use as required.

From Eqs. (B13) and (B18), we then have

$$S_l(2,r)=\tfrac{1}{2}Q_l^{(a)}(R_2,r)+Q_l^{(b)}(R_2,r)+\tfrac{1}{2}Q_l^{(c)}(R_2,r), \tag{B19}$$

where

$$Q_l^{(a)}(R_2,r)=\frac{1}{R_2r}\int\frac{[s(\rho)]^2}{\rho}I_l^{(a)}(r,\rho,R_2)d\rho, \tag{B20a}$$

$$Q_l^{(b)}(R_2,r)=\frac{1}{R_2r}\int\frac{s(\rho)g(\rho)}{\rho}I_l^{(b)}(r,\rho,R_2)d\rho, \tag{B20b}$$

$$Q_l^{(c)}(R_2,r)=\frac{1}{R_2r}\int\frac{[g(\rho)]^2}{\rho}I_l^{(c)}(r,\rho,R_2)d\rho. \tag{B20c}$$

These integrations are carried out during each iteration using Simpson's rule[11] with step size $h=0.05$ Å.

Now that we have $S_l(2,r)$, we proceed to $S_l(3,r)$. Rotate the coordinate systems centered at lattice sites No. 1 and No. 3, keeping them parallel, in such a fashion that with reference to the rotated coordinate-system lattice site No. 3 has the same coordinates as

[10] H. Goldstein, *Classical Mechanics* (Addison-Wesley Publishing Company, Reading, Massachusetts, 1950).

[11] M. G. Salvadori and M. L. Baron, *Numerical Methods in Engineering* (Prentice-Hall, Inc., Englewood Cliffs, New Jersey, 1961).

site No. 2 had with reference to the coordinate system before rotation. This rotation is clearly a cubic-symmetry operation, and hence the functional forms of the KH with respect to the new coordinates remain unchanged. Also, the magnitudes $r^{(3)}$ and $r$ remain unchanged by this (or any) rotation. Thus we see that $S_l(3,r)$ is given by the same integral as $S_l(2,r)$, Eq. (B13). Similarly, we get the same contribution for each of the other members of the first shell. Hence, if $R$ is the magnitude of the distance of any member of the first shell from lattice site No. 1, the total contribution of the first shell is

$$\sum_{j=2}^{9} S_l(j,r)=8[\tfrac{1}{2}Q_l^{(a)}(R,r)+Q_l^{(b)}(R,r)+\tfrac{1}{2}Q_l^{(c)}(R,r)]. \quad \text{(B21)}$$

For the set of second-nearest neighbors ($j=10$ to 15 inclusively), the rotation of coordinates so that $z\rightarrow\bar{z}$ where $\bar{z}$ and $\mathbf{R}_j(10\leq j\leq 15)$ are collinear, is a cubic-symmetry operation, and the KH thus remain invariant in functional form. (Of course, for one of the members of the second shell no rotation at all is required to make $z$ and $\mathbf{R}_j$ collinear.) This shell is then dealt with analogously to the first shell.

In the next 11 shells (we do 13 shells in all) we make the following two approximations: First, that these shells contain spherically symmetric wave functions at each lattice site, and, second, that the lattice sites for each shell ($\geq$ third) are spread out uniformly over a sphere. This latter condition is equivalent to setting

$$S_l(r)=0, \quad l\geq 4, \quad \text{shells}\geq\text{third}. \quad \text{(B22)}$$

These approximations should have negligible effect on the results since each particle, and in particular particle No. 1, should be rigorously confined to its own lattice cell, and hence should not be significantly affected by the detailed structure of the outer shells ($\geq$ third).

Returning to the wave functions, we use only $u_0(r)$ and set $u_4(r)=0$. Then, of course, $u_0(r)$ must be renormalized to have the same normalization as the original total wave function. Defining therefore

$$C_0^{-2}=4\pi\int[s(r)]^2dr, \quad \text{(B23)}$$

we then have as the contribution of any shell$\geq$third at distance $R$ from lattice site No. 1,

$$\sum_{\text{shell}} S_l(j,r)=\frac{N_s C_0^2}{2rR}\int\frac{[s(\rho)]^2}{\rho}d\rho, \quad \text{(B24)}$$

where $N_s$ is the number of lattice sites in the shell.

The contributions from all the shells up to 13 are added to obtain $S_l(r)$ for $l=0, 4, 6, 8$, for those values of $r$ (in steps of $h=0.05$ Å) which are subsequently required.

Once we have $J_l(r_1,r_2)$ and $S_l(r_2)$, we calculate $W_l(r_1)$ by using Simpson's Rule to evaluate

$$W_l(r_1)=\frac{4\pi}{2l+1}\int S_l(r_2)J_l(r_1,r_2)r_2^2dr_2. \quad \text{(B25)}$$

### Solution of Coupled Equations

In this section we review briefly the methods used to solve numerically the coupled set of Eqs. (3.24) which are of the form

$$\frac{d^2s(r)}{dr^2}+[A(r)+\epsilon]s(r)+B(r)g(r)=0, \quad \text{(B26a)}$$

$$\frac{d^2g(r)}{dr^2}+[C(r)+\epsilon]g(r)+D(r)s(r)=0. \quad \text{(B26b)}$$

We follow the methods suggested by Fox,[12] and the reader is referred to Ref. 12 for more complete details. Throughout the following we use the notation

$$r_m\equiv mh, \quad \text{(B27)}$$

where $h$ is some given step size, and $m$ is an integer.

As explained subsequently the boundary conditions we use are

$$s(r_0)=g(r_0)=0, \quad \text{(B28a)}$$

$$s(r_n)=g(r_n)=0, \quad \text{(B28b)}$$

where

$$r_n=\tfrac{1}{2}A, \quad \text{(B29)}$$

where $A$ is the nearest-neighbor distance.

The boundary condition at the origin is chosen to insure that the wave function $\psi(\mathbf{r})$ remains finite as $r\rightarrow 0$. In the case of the $LJ$ potential, since $v_{LJ}(r)\rightarrow\infty$ as $r\rightarrow 0$, we see at once from the Hartree potential, Eq. (3.14), that any overlap of the single-particle wave functions is rigorously forbidden, and thus we have the boundary condition at $r_n=\frac{1}{2}A$.

Now, using Noumerov's method[11] for the derivatives, we start out from the origin in steps of $h=0.05$ Å, with the first two steps being given by

$$s(r_0)=0, \qquad g(r_0)=0, \quad \text{(B30a)}$$

$$s(r_1)=0.001, \quad g(r_1)=p, \quad \text{(B30b)}$$

where $p$ is a parameter whose value may not be fixed arbitrarily. It arises since $s(r_1)$ fixes the normalization of the solution, and hence we cannot choose $g(r_1)$ arbitrarily. Thus, in addition to the functions $s(r)$, $g(r)$, Eqs. (B26) must be solved for the parameters $\epsilon$, $p$. We make an initial guess at $\epsilon$ and $p$, the first guess for $\epsilon$ being $\epsilon=W_0(r_0)$, and starting from Eq. (B30) we inte-

[12] Leslie Fox, in *Boundary Problems in Differential Equations*, edited by R. E. Langer (The University of Wisconsin Press, Madison, Wisconsin, 1960).

grate out to $r_n$. In general this will not give $s(r_n)=g(r_n)=0$ as required by the boundary conditions, and from the mismatch at $r_n$ we are able to determine an improved $\epsilon$ and $p$ for the next trial. We repeat the procedure until our iterations for $\epsilon$ and $p$ "settle down."

Experiment has shown[12] that the above method does not produce good eigenfunctions throughout the whole range of $r$. The eigenfunctions are important in our case since they are used to get the Hartree potential for the subsequent major iteration. Hence, we use the above method to get a rough idea of the correct eigenvalues and, using these as starting values, we use the following method (also suggested by Fox) to obtain the final results. We integrate both forwards and backwards and our aim is to have the forward and backward solutions meet at some central point $r_c$ with the same height and slope. We keep the same forward boundary conditions as before and, in addition, we take as the starting conditions for our backward solution

$$s(r_n)=0, \qquad g(r_n)=0, \tag{B31a}$$

$$s(r_{n-1})=0.001, \quad g(r_{n-1})=q. \tag{B31b}$$

The backward solution must be associated with a factor $k$ to be determined so that the normalization of the backward solution is the same as that of the forward solution. After an initial guess, the new $\epsilon$, $p$, $q$, and $k$ for the next trial are determined from the conditions required in order that the forward and backward solutions meet at $r_c$ with no discontinuity. This procedure is repeated until the iterations "settle down" for $\epsilon$ in particular, and this, then, is the solution for the eigenfunction $[s(r),g(r)]$ and the single-particle energy $\epsilon_0$. By "settle down" we mean typically in our calculations that we continue iterating until the change is less than 0.5% of the last-obtained $\epsilon$.

PHYSICAL REVIEW VOLUME 154, NUMBER 1 5 FEBRUARY 1967

# Method of Solution of the Percus-Yevick, Hypernetted-Chain, or Similar Equations

R. J. BAXTER

*Research School of Physical Sciences, The Australian National University, Canberra, Australia*

(Received 25 August 1966; revised manuscript received 17 October 1966)

It is shown that if the direct correlation function $c(r)$ in classical statistical mechanics vanishes beyond a range $R$, then the equation relating it to the radial distribution function may be used to derive a further equation which involves both functions only over the range $(0,R)$. The analytic solution of the Percus-Yevick (PY) equation for hard spheres follows as an immediate consequence, and since $c(r)$ normally tends rapidly to zero with increasing $r$, it is expected that the result should be of use in numerical solutions of PY, convolution-hypernetted-chain, or similar approximations.

## I. INTRODUCTION

IN the classical statistical mechanics of homogeneous fluids various approximations have been proposed which involve the direct correlation function $c(\mathbf{x})$, defined by

$$h(\mathbf{x})=c(\mathbf{x})+\rho\int d\mathbf{y}\, c(\mathbf{y})h(\mathbf{x}-\mathbf{y}), \tag{1}$$

where $\rho$ is the particle density and $h(\mathbf{x})$, the indirect correlation function, is defined in terms of the radial distribution function $g(\mathbf{x})$ by

$$h(\mathbf{x})=g(\mathbf{x})-1. \tag{2}$$

In particular, if $\phi(\mathbf{x})$ is the interaction potential and $\beta$ is the Boltzmann factor $(kT)^{-1}$, the Percus-Yevick (PY) approximation[1,2] supplements (1) and (2) with the approximate relation

$$e^{-\beta\phi(\mathbf{x})}c(\mathbf{x})=\{e^{-\beta\phi(\mathbf{x})}-1\}g(\mathbf{x}), \tag{3a}$$

while the convolution-hypernetted-chain (CHNC) approximation[3,4] supplements them with

$$c(\mathbf{x})=h(\mathbf{x})-\log g(\mathbf{x})-\beta\phi(\mathbf{x}). \tag{3b}$$

In solving any such approximation it is found that the direct correlation function tends to zero with increasing $|\mathbf{x}|$ much more rapidly than the indirect correlation function[5]; for instance, the PY relation (3a) shows that $c(\mathbf{x})$ vanishes exactly outside the range of $\phi(\mathbf{x})$, while the CHNC relation (3b) predicts that it behaves as $\frac{1}{2}h^2(\mathbf{x})$ when $h(\mathbf{x})$ is small. It is therefore unfortunate that in considering the solutions of the equations the

[1] J. K. Percus and G. J. Yevick, Phys. Rev. **110**, 1 (1958).
[2] J. K. Percus, Phys. Rev. Letters **8**, 462 (1962).
[3] J. M. J. Van Leeuwen, J. Groeneveld, and J. de Boer, Physica **25**, 792 (1959).
[4] T. Morita and K. Hiroike, Progr. Theoret. Phys. (Kyoto) **23**, 1003 (1960).
[5] L. Goldstein, Phys. Rev. **100**, 981 (1955).